Electronic Supplementary Material (ESI) for Chemical Science.

Supplementary Information for

Regioisomer Effects of [70]Fullerene Mono-adduct Acceptors in Bulk Heterojunction Polymer Solar Cells

Tomokazu Umeyama,[a] Tetsushi Miyata,[a] Andreas C. Jakowetz,[b] Sho Shibata,[a] Kei Kurotobi,[c]
Tomohiro Higashino,[a] Tomoyuki Koganezawa,[d] Masahiko Tsujimoto,[c] Simon Gélinas,[b]
Wakana Matsuda,[a] Shu Seki,[a] Richard H. Friend,*[b] and Hiroshi Imahori*[ac]

[a] *Department of Molecular Engineering, Graduate School of Engineering, Kyoto University, Nishikyo-ku, Kyoto, 615-8510, Japan*

[b] *Cavendish Laboratory, University of Cambridge, J J Thomson Avenue, Cambridge, CB3 0HE, United Kingdom*

[c] *Institute for Integrated Cell-Material Sciences (WPI-iCeMS), Kyoto University, Nishikyo-ku, Kyoto 615-8510, Japan*

[b] *Japan Synchrotron Radiation Research Institute, 1-1-1, Kouto, Sayo-cho, Sayo-gun, Hyogo 679-5198, Japan*

E-mail: rhf10@cam.ac.uk, imahori@scl.kyoto-u.ac.jp

1. Instruments

Fullerene derivative isomers separation was conducted by Shimadzu Prominence Modular HPLC with Nacalai Tesque cosmosil buckyprep (20 × 250 mm); eluent, toluene; flow rate, 10 mL min^{-1}; detection, 380 nm. ^{1}H NMR spectra and ^{13}C NMR were measured with a JEOL JNM-EX400 NMR spectrometer, and a Bruker AVANCE 500 spectrometer. Attenuated total reflectance (ATR) FT-IR spectra were recorded on a Themo Fisher Scientific Nicolet 6700 FT-IR. High-resolution mass spectra were measured on a Thermo Fisher Scientific EXACTIVE (ESI and APCI) and LTQ orbitrp XL (MALDI). UV-vis absorption spectra were obtained on a Perkin Elmer Lambda 900UV/vis/NIR spectrometer. Steady-state fluorescence spectra were recorded on a HORIBA SPEX Fluoromax-3 spectrofluorometer. Atomic force microscopy (AFM) analyses were carried out with an Asylum Technology MFP-3D-SA in the AC mode. Thermogravimetric analysis (TGA) measurements were conducted with a SHIMADZU TG-60 under flowing nitrogen at a scan rate of 10 ˚C min^{-1}. Differential scanning calorimetry (DSC) analysis was made on a SHIMADZU DSC-60 at a scan rate of 10 ˚C min^{-1}. Cyclic voltammetry (CV) and differential pulse voltammetry (DPV) measurements were performed using an ALS 630A electrochemical analyzer in *o*-dichlorobenzene/acetonitrile mixture (v:v=5:1) containing 0.1 M tetra-*n*-butylammonium hexafluorophosphate (Bu_4PF_6) as a supporting electrolyte.

2. Synthesis and isomer separation

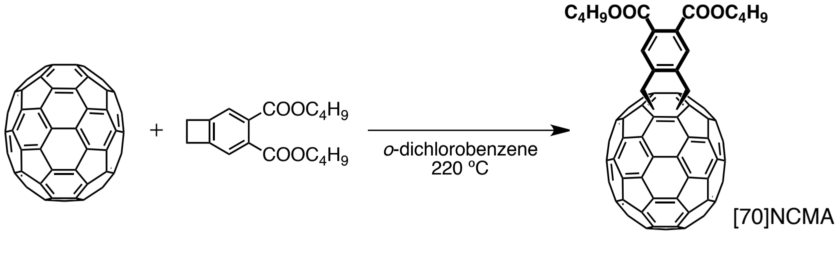

2.1. Synthesis of [70]NCMA. 4,5-Bis(butoxycarbonyl)benzocyclobutene (122 mg, 0.400 mmol) and C_{70} (300 mg, 0.357 mmol) were dissolved in *o*-dichlorobenzene (60 mL) in a 200 mL round bottom flask. The solution was degassed, substituted by Ar and then heated at 220 °C for 38 h in a closed system. After cooling to room temperature, the reaction mixture was charged on a silica gel column. The unreacted C_{70}, the corresponding mono-adduct ([70]NCMA), and multi-adducts were separated by the column chromatography with toluene/hexane (v/v = 1/1) and then toluene as eluents. A total 222 mg of [70]NCMA as a regioisomer mixture was obtained (yield 54.4%) and 61.9 mg of C_{70} (20.6 %) was recovered.

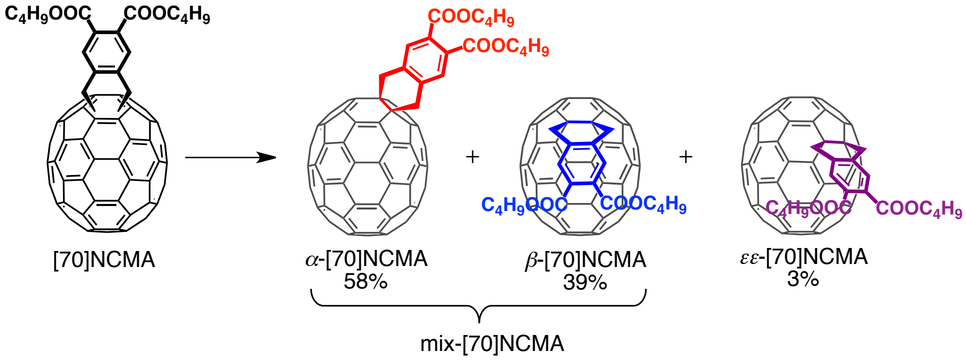

2.2. Separation and purification of [70]NCMA isomers. Separation of a regioisomer mixture of [70]NCMA (220.0 mg) was accomplished by HPLC with a Buckyprep column at 50 °C using toluene as an eluent. *α*-type isomer (*α*-[70]NCMA, 128.8 mg, yield 58%), *β*-type isomer (*β*-[70]NCMA, 86.6 mg, yield 39%), and *εε*-isomer (reacted at [6,5]-bond in between *ε*-type [6,6]-bonds,[S1] 6.6 mg, yield 3%) were obtained. Due to the low yield of *εε*-[70]NCMA its electrochemical and photovoltaic properties could not be evaluated. We also prepared a sample, mix-[70]NCMA, just by removing *εε*-[70]NCMA from [70]NCMA, that is, mix-[70]NCMA consists of *β*-[70]NCMA and *α*-[70]NCMA with the ratio of 39 : 58.

α-[70]NCMA: ^1H NMR ($C_2D_2Cl_4$, 393 K, 400 MHz): δ 7.98 (s, 1H), 7.75 (s, 1H), 4.44-4.37 (4H), 4.25 (2H), 3.85 (2H), 1.90-1.76 (4H), 1.61-1.46 (4H), 1.10-1.00 (6H). ^{13}C NMR ($C_2D_2Cl_4$, 393 K, 400 MHz): δ 166.95, 166.88, 160.44, 154.50, 151.16, 151.12, 151.09, 150.85, 150.43, 150.40, 149.68, 149.62, 149.34, 149.22, 149.17, 148.76, 148.53, 147.45, 147.16, 146.79, 146.74, 146.71, 146.01, 145.91, 145.51, 142.89, 142.76, 142.61, 140.06, 139.81, 139.65, 136.70, 133.57, 133.54, 131.95, 131.92, 131.16, 131.03, 131.00, 127.82, 127.72, 65.33, 65.27, 58.43, 56.89, 44.2, 40.62, 30.28, 30.21 18.72, 18.66, 13.12, 13.06. HRMS (p APCI): found, 1145.1739; calcd $(M+H)^+$, 1145.1747. UV-vis ($CHCl_3$): λ/nm (ε/M^{-1} cm^{-1}) 397 (25600), 461 (19400). IR (ATR): ν_{max}/cm^{-1} 2952, 2927, 2866, 2342, 2185, 2106, 2086, 1997, 1724, 1618, 1571, 1453, 1427, 1330, 1279, 1224, 1170, 1122, 1032, 961, 899, 845, 795, 672. Crystallographic data: $C_{88}H_{24}O_4{\cdot}0.5(C_6H_{14})$, M_r = 1188.16, monoclinic, $P2_1/n$ (No.14), a = 10.1470(16), b = 23.719(4), c = 21.227(4) Å, β = 102.193(2)°, V = 4993.6(14) Å^3, ρ_{calcd} = 1.580 g cm^{-3}, Z = 4, R_1 = 0.0616 [$I > 2\sigma(I)$], wR_2 = 0.1624 (all data), GOF = 1.056.

β-[70]NCMA: ^1H NMR ($C_2D_2Cl_4$, 393 K, 400 MHz): δ 7.72 (s, 2H), 4.38 (4H), 3.80 (4H), 1.81 (4H), 1.51 (4H), 1.04 (6H). ^{13}C NMR ($C_2D_2Cl_4$, 393 K, 400 MHz): δ 167.17, 154.88, 154.67, 153.55, 151.61, 150.58, 150.19, 149.23, 148.98, 148.89, 148.10, 147.95, 147.76, 147.07, 146.92, 146.82, 146.68, 146.48, 146.43, 146.05, 145.65, 145.47, 145.11, 144.89, 144.58, 144.29, 143.76, 143.50, 143.03, 142.23, 141.34, 140.50, 140.27, 132.40, 132.13, 132.01, 131.27, 131.23, 127.83, 125.71, 65.55, 55.38, 43.32, 30.50, 18.96, 13.37. HRMS (p APCI): found, 1145.1741; calcd $(M+H)^+$,1145.1747. UV-vis ($CHCl_3$): λ/nm (ε/M^{-1} cm^{-1}) 363 (27500), 398 (24000), 435 (18700). IR (ATR): ν_{max}/cm^{-1} 3055, 2951, 2866, 2729, 2351, 2331, 2281, 2113, 2083, 2052, 1974, 1947, 1724, 1618, 1570, 1531, 1403, 1328, 1280, 1211, 1166, 1120, 1071, 1032, 962, 895, 848, 793, 677. Crystallographic data: $C_{88}H_{24}O_4$, M_r = 1145.07, tetragonal, $P4_2/mbc$ (No.135), a = 26.123(4), b = 26.123(4), c = 14.146(2) Å, V = 9653(3) Å^3, ρ_{calcd} = 1.576 g cm^{-3}, Z = 8, R_1 = 0.1177 [$I > 2\sigma(I)$], wR_2 = 0.4472 (all data), GOF = 1.077.

$\varepsilon\varepsilon$-[70]NCMA: ^1H NMR ($C_2D_2Cl_4$, 393 K, 400 MHz): δ 7.64 (s, 2H), 4.36 (t, 4H, J=6.8 Hz), 3.78 (d, 2H, J=15 Hz), 3.23 (t, 2H, J=14 Hz), 1.80 (t, 4H, J=6.8 Hz), 1.54-1.48 (m, 4H), 1.05-1.00 (m, 6H). ^{13}C NMR ($C_2D_2Cl_4$, 393 K, 500 MHz): δ 166.99, 155.45, 153.98, 151.12, 149.72, 149.19, 149.11, 148.54, 148.26, 147.89, 147.72, 147.41, 146.97, 146.69, 146.20, 146.17, 146.01, 145.81, 145.78, 145.33, 145.03, 144.17, 143.57, 143.42, 140.87, 140.25, 140.03, 139.57, 139.39, 139.13, 135.10, 134.61, 132.83, 132.73, 131.94, 131.75, 128.44, 127.92, 65.53, 44.01, 56.40, 30.53, 19.01, 13.42. HRMS (p APCI): found, 1145.1732; calcd $(M+H)^+$, 1145.1747. UV-vis ($CHCl_3$): λ/nm (ε/M^{-1} cm^{-1}) 322 (40800), 371 (18500), 395 (17100), 513 (8800), 647 (2800), 758 (747). IR (ATR): ν_{max}/cm^{-1} 3469, 2961, 2931, 2869, 2367, 2338, 2248, 2226, 2168, 2146, 2077, 2049, 1991, 1974, 1961, 1723, 1574, 1533, 1463, 1392, 1331, 1281, 1230, 1219, 1198, 1166, 1125, 1090, 1079, 1035, 949, 792, 737.

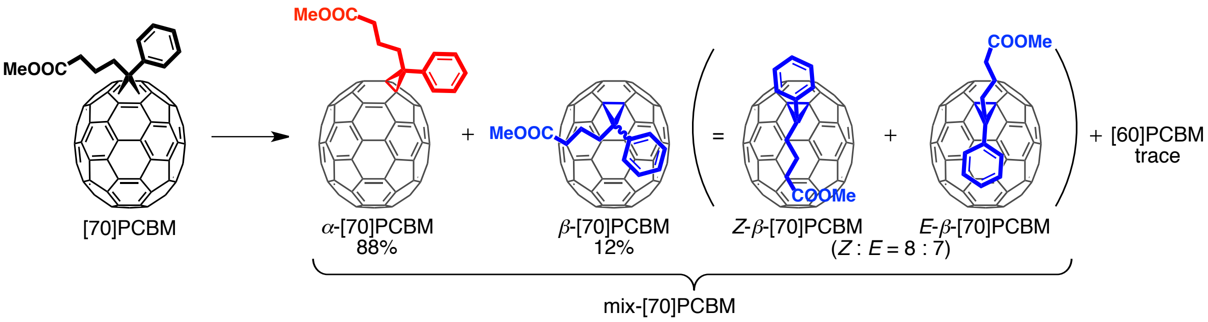

2.3. Separation and purification of [70]PCBM isomers. Separation of a regioisomer mixture of [70]PCBM (60.0 mg) was accomplished by HPLC with a Buckyprep column at 50 ºC using toluene as an eluent. *α*-type isomer (*α*-[70]PCBM, 52.6 mg, yield 87.7%), *β*-type isomer (*β*-[70]PCBM, 7.2 mg, yield 12.0%), and an impurity [60]PCBM (0.2 mg, 0.3%) were obtained. Although diastereomers of *β*-[70]PCBM, i.e. *Z*-*β*-[70]PCBM and *E*-*β*-[70]PCBM, could not be separated, signals in ^1H NMR spectra are discernible, indicating that the ratio of *Z* : *E* is 8 : 7.

α-[70]PCBM: ^1H NMR (CS_2:CD_2Cl_2=4:1, r.t., 400 MHz): δ 7.84 (s, 2H), 7.49-7.45 (m, 2H), 7.40-7.38 (m, 1H), 3.60 (m, 3H), 2.42-2.31 (m, 4H), 2.14-1.99 (m, 2H). ^{13}C NMR (CS_2:CD_2Cl_2=1:1, r.t., 400 MHz): δ 172.55, 156.63, 155.94, 152.92, 152.70, 152.16, 151.88, 151.81, 151.55, 151.50, 151,26, 151.20, 150.11, 150.07, 149.94, 149.86, 149.84, 149.81, 149.32, 149.28, 149.24, 149.20, 149.12, 149.05, 148.83, 148.59, 148.47, 148.24, 148.20, 148.15, 148.09, 147.71, 147.54, 147.01, 146.82, 146.70, 146.59, 146.42, 146.42, 146.34, 145.26, 144.84, 144.67, 144.62, 144.48, 144.37, 144.10, 144.02, 143.41, 143.28, 142.48, 142.30, 142.06, 141.76, 140.92, 140.09, 139.44, 138.56, 137.95, 134.70, 134.51, 133.51, 133.50, 132.28, 131.60, 131.47, 131.45, 131.43, 131.38, 131.26, 131.17, 129.01, 128.35, 72.50, 70.41, 51.83, 36.65, 34.85, 34.25, 22.56. HRMS (p ESI): found, 1030.09888; calcd $(M)^+$, 1030.09883. UV-vis ($CHCl_3$): λ/nm (ε/M^{-1} cm^{-1}) 355 (25100), 372 (26500), 400 (19700), 462 (21800). IR (ATR): ν_{max}/cm^{-1} 3027, 2943, 2522, 2345, 2127, 2089, 2049, 2024, 1879, 1738, 1603, 1569, 1538, 1494, 1453, 1429, 1330, 1249, 1035, 795, 750, 701, 674, 644, 579, 535, 460. Crystallographic data: $C_{82}H_{14}O_2$, $M_r = 1030.93$, monoclinic, $P2_1/c$ (No.14), $a = 10.9852(7)$, $b = 20.5331(14)$, $c = 19.4487(13)$ Å, $\beta = 91.193(6)°$, $V = 4385.9(5)$ $Å^3$, $\rho_{calcd} = 1.561$ g cm^{-3}, $Z = 4$, $R_1 = 0.1491$ [$I > 2\sigma(I)$], $wR_2 = 0.4125$ (all data), GOF = 1.079.

β-[70]PCBM: ^{1}H NMR (Z-β-[70]PCBM, CS_2:CD_2Cl_2=4:1, r.t., 400 MHz): δ 7.72-7.70 (m, 2H), 7.52-7.44 (m, 3H), 3.42 (s, 3H), 2.31-2.03 (m, 4H), 1.74-1.70 (m, 2H). ^{1}H NMR (E-β-[70]PCBM, CS_2:CD_2Cl_2=4:1, r.t., 400 MHz): δ 7.35-7.34 (m, 2H), 7.17-7.14 (m 3H), 3.64 (s, 3H), 2.42-2.40 (m, 4H), 1.95-1.91 (m, 2H). ^{13}C NMR (CS_2:CD_2Cl_2=1:1, r.t., 400 MHz): δ 172.59 (ascribed to Z-isomer, denoted as z), 172.29 (ascribed to E-isomer, denoted as e), 153.90, 151.09, 150. 70, 150.62, 150.45, 150.35, 150.31, 150.26, 150.15, 150.15, 150.10, 150.74, 149.91, 149.80, 149.51, 149.33, 149.18, 149.02, 148.91, 148.88, 148.79, 148.62, 147.92, 147.90, 147.88, 147.87, 147.78, 147.72, 147.62, 147.52, 147.49, 147.21, 146.92, 146.62, 146.57, 146.54, 146.24, 146.22, 146.05, 145.61, 145.52, 145.31, 145.22, 144.97, 144.91, 144.87, 144.26, 143.82, 143.77, 143.50, 143.42, 143.38, 143.18, 142.52, 142.35, 142.27, 141.92, 140.39, 138.72, 137.37, 133.19, 132.94, 132.87, 132.51, 132.36, 132.16, 131.91, 131.87, 131.26, 129.78, 129.40, 129.07, 129.05, 128.72, 128.56, 127.72, 126.16, 66.21 (z), 65.94 (e), 51.88 (e), 51.68 (z), 38.57 (z), 38.15 (e), 36.01 (z), 34.28 (z), 34.13 (e), 33.94 (e), 22.93 (z), 22.49 (e). HRMS (p MALDI): found, 1030.09912; calcd $(M)^+$, 1030.

09883. UV-vis ($CHCl_3$): λ/nm (ε/M^{-1} cm^{-1}) 393 (29200), 443 (18900). IR (ATR): ν_{max}/cm^{-1} 3057, 3021, 2986, 2940, 2925, 2859, 2839, 2632, 2569, 2462, 2403, 2347, 2332, 2218, 2197, 2179, 2144, 2124, 2088, 1956, 1936, 1735, 1601, 1569, 1536, 1493, 1428, 1333, 1246, 1076, 1034, 947, 913, 841, 795, 701, 674.

3. Theoretical calculations

All calculations were carried out using the Gaussian 09 program.[S2] All structures were fully optimized without any symmetry restriction. The calculations were performed by the density functional theory (DFT) method with restricted B3LYP (Becke's three-parameter hybrid exchange functionals and the Lee-Yang-Parr correlation functional) level, employing a basis set 6-31G* for C, H and O. Absolute ^{1}H shielding values were obtained with the GIAO method at the B3LYP/6-31G* level. The ^{1}H chemical shift values were calculated relative to $CHCl_3$ (δ = 7.26 ppm, absolute shielding: 24.94 ppm).

4. GISAXS and GIWAXS

Samples were prepared by spin-coating the PCDTBT:fullerene solution on the ITO/PEDOT:PSS substrate as conducted in the PSC device fabrications. GISAXS and GIWAXS measurements were conducted at the SPring-8 on beamline BL46XU. For the GISAXS measurements, the sample was irradiated at a fixed incident angle on the order of 0.12° through a Huber diffractometer with an X-ray energy of 8.000 keV (X-ray wavelength λ = 0.155 nm), and the GISAXS patterns were recorded with a 2D image detector (Pilatus 2 M) with the sample-to-detector distances of 3022 mm. GISAXS intensity profiles in the lower-q region contributed by fullerene aggregates in the PCDTBT:fullerene blend films were modeled with Debye-Anderson-Brumberger (DAB) equation,[S3,S4]

$$I(q) = \frac{A}{\{1 + (qL)^2\}^2}$$

with scattering intensity I, constant A, scattering vector q, and correlation length L. For the GIWAXS measurements, the sample was irradiated at a fixed incident angle on the order of 0.12° through a Huber diffractometer with X-ray energy of 12.398 keV (X-ray wavelength λ = 0.10002 nm), and the GIWAXS patterns were recorded with a 2D image detector (Pilatus 300 K) with the sample-to-detector distances of 173.8 mm.

5. Time-resolved microwave conductivity measurements. The nanosecond laser pulses from an Nd:YAG laser (third harmonic generation, THG (355 nm) from Spectra Physics, INDI-HG, FWHM 4 ns) was used as excitation source. The excitation density was 4.6×10^{15} photons cm^{-2}. The resonant frequency and the microwave power were set at ~9.1 GHz and 5 mW, respectively. The time-resolved microwave conductivity (TRMC) signal from a diode was recorded on a digital oscilloscope (Tektronix, TDS 3032B). The transient photoconductivity ($\Delta\sigma$) of the samples is related to the reflected microwave power ($\Delta P_\mathrm{r}/P_\mathrm{r}$) and sum of the mobilities of charge carriers via:

$$\langle \Delta\sigma \rangle = \frac{1}{A}\frac{\Delta P_r}{P_r} \qquad (1)$$

$$\Delta\sigma = e\phi N \sum \mu \qquad (2)$$

where A is the sensitivity factor, e is the elementary charge of electron, ϕ is the photo-carrier generation yield (quantum efficiency), N is the number of absorbed photons per unit volume, and $\Sigma\mu$ is the sum of mobility for the negative and positive carriers. For the sample preparations, fullerene single component films were formed on quartz substrates.

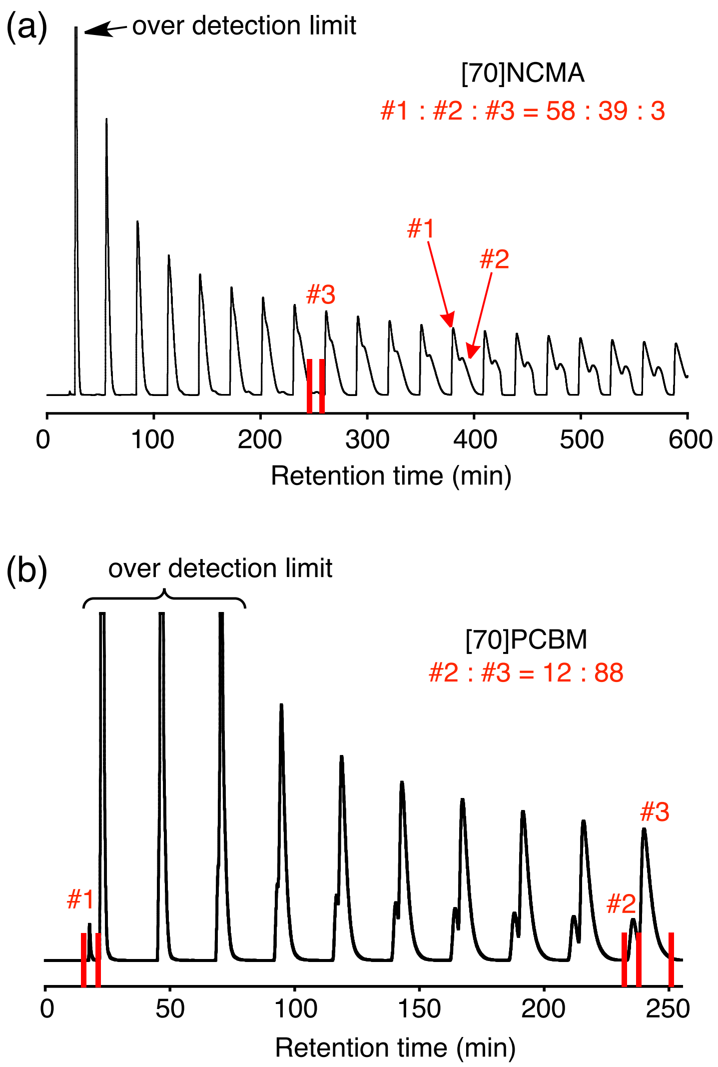

Fig. S1 (a) HPLC profile of [70]NCMA. The weight ratio of the three fractions (#1 : #2 : #3) after the separation was 58 : 39 : 3. The third fraction was separated at once as indicated in the HPLC profile. The first and second fractions were collected gradually with repeated recycling. The first, second, and third fractions were assigned to α-[70]NCMA, β-[70]NCMA, and $\varepsilon\varepsilon$-[70]NCMA (reacted at [6,5]-bond in between ε-type [6,6]-bonds),[S1] respectively. (b) HPLC profile of [70]PCBM. The weight ratio of the main fractions (#2 : #3) after the separation was 12 : 88. The first, second, and third fractions were assigned to [60]PCBM, β-[70]PCBM, and α-[70]PCBM, respectively.

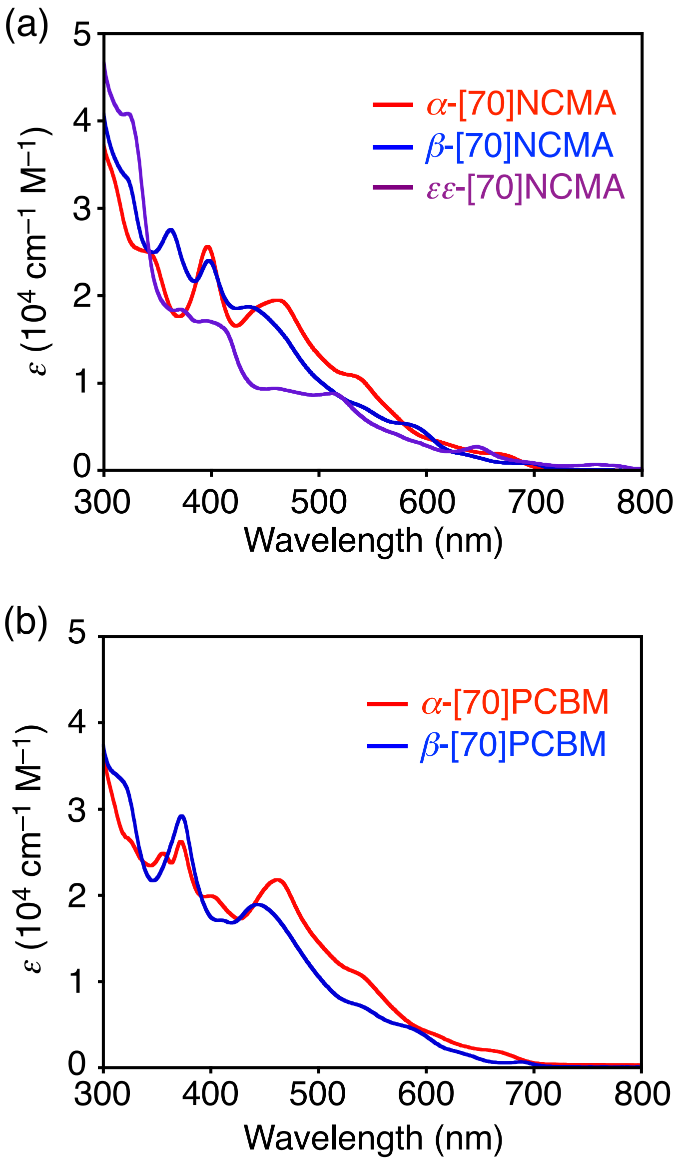

Fig. S2 UV-vis absorption spectra of (a) *α*-[70]NCMA (red), *β*-[70]NCMA (blue), and *εε*-[70]NCMA (purple) and (b) *α*-[70]PCBM (red) and *β*-[70]PCBM (blue) in $CHCl_3$.

(a)

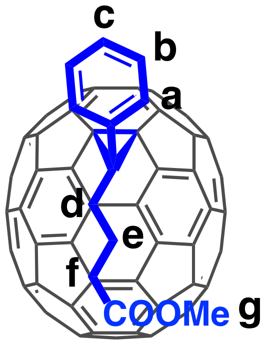

Z-*β*-[70]PCBM

Chemical Shift / ppm
a: 7.84
b: 7.46
c: 7.41
d: 2.07
e: 1.92
f : 1.55
g: 3.43

(b)

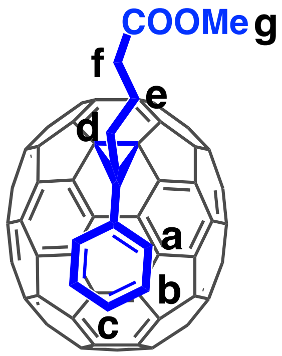

E-*β*-[70]PCBM

Chemical Shift / ppm
a: 7.46
b: 7.16
c: 7.12
d: 2.16
e: 2.11
f : 2.26
g: 3.68

Fig. S3 Chemical structures and simulated chemical shifts of (a) *Z*-*β*-[70]PCBM and (b) *E*-*β*-[70]PCBM. The simulation was conducted with the GIAO method at the B3LYP/6-31G* level. The simulated chemical shifts are largely consistent with the experimental values and thus the ratio is *Z*-isomer : *E*-isomer = 8 : 7.

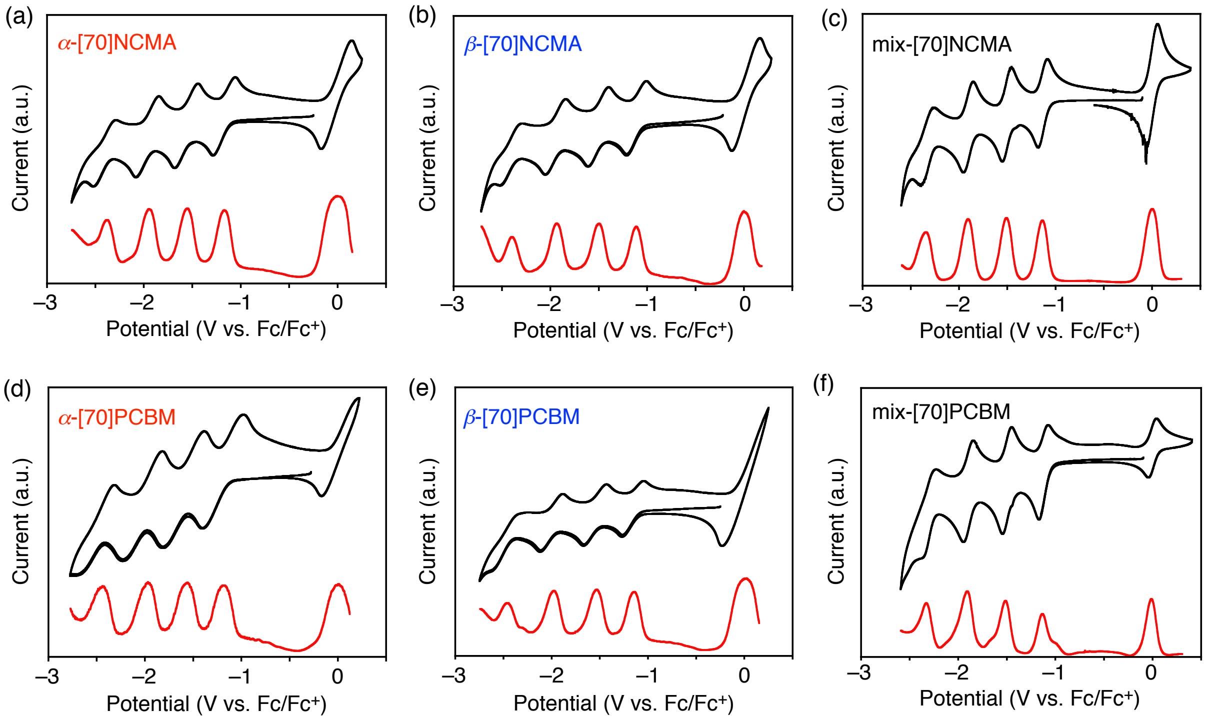

Fig. S4 Cyclic voltammograms (black) and differential pulse voltammograms (red) of (a) *α*-[70]NCMA, (b) *β*-[70]NCMA, (c) mix-[70]NCMA, (d) *α*-[70]PCBM, (e) *β*-[70]PCBM, and (f) mix-[70]PCBM measured in *o*-dichlorobenzene/acetonitrile mixture (v:v=5:1) containing 0.1 M Bu_4NPF_6. Sweep rate: 0.1 V s^{-1}; reference electrode, Ag/$AgNO_3$ (0.01 M $AgNO_3$, 0.09 M Bu_4PF_6 in acetonitrile). Ferrocene (Fc) was also added in the solution as the internal standard.

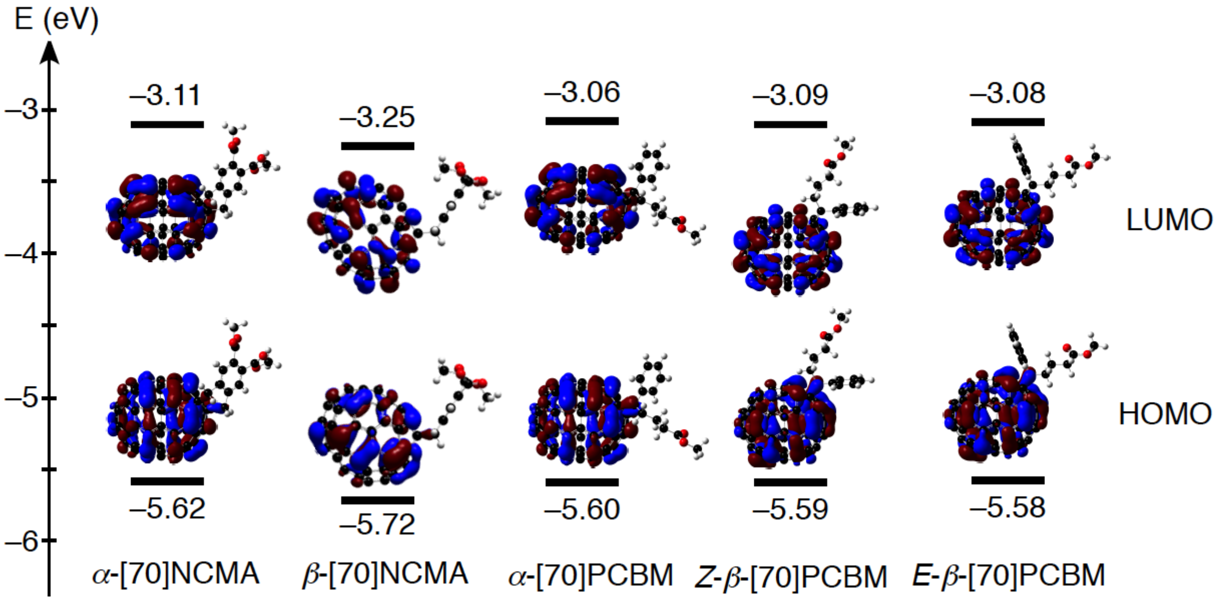

Fig. S5 Optimized geometries, HOMO/LUMO electron density distributions, and energy levels of *α*-[70]NCMA, *β*-[70]NCMA, *α*-[70]PCBM, *Z*-*β*-[70]PCBM, and *E*-*β*-[70]PCBM simulated by DFT calculations using B3LYP/6-31G* model. Butyl groups in *α*-[70]NCMA and *β*-[70]NCMA are replaced by methyl groups to reduce the calculation cost.

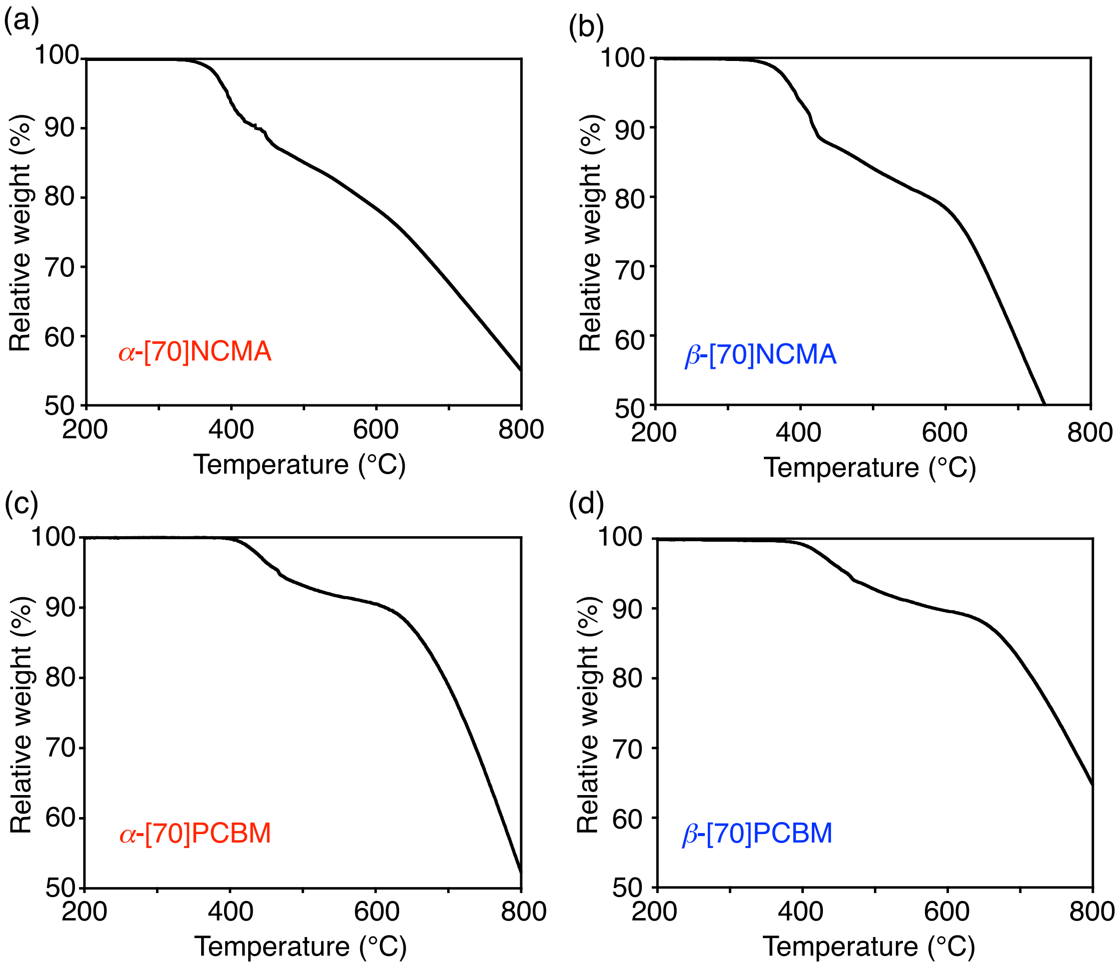

Fig. S6 TGA curves of (a) *α*-[70]NCMA, (b) *β*-[70]NCMA, (c) *α*-[70]PCBM, and (d) *β*-[70]PCBM. The measurements were performed under flowing nitrogen at a scan rate of 10 °C min^{-1}.

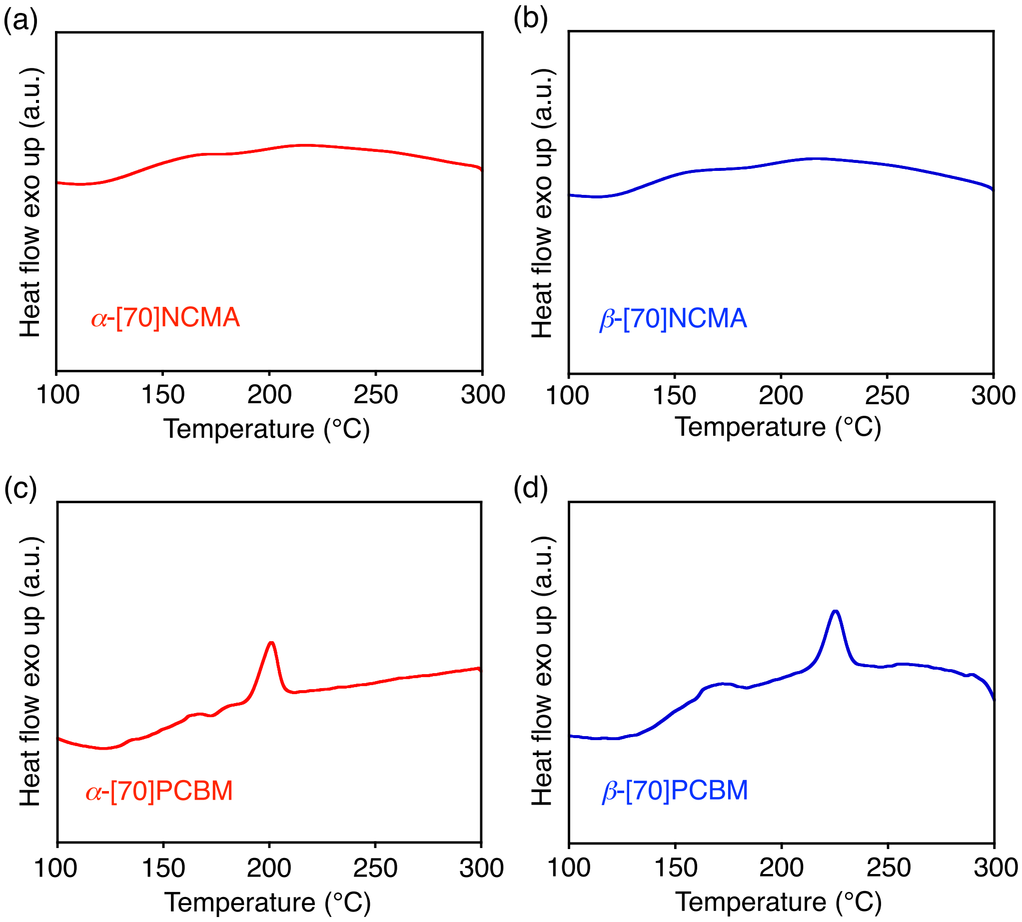

Fig. S7 DSC curves of (a) α-[70]NCMA, (b) β-[70]NCMA, (c) α-[70]PCBM, and (d) β-[70]PCBM. The measurements were performed under flowing nitrogen at a scan rate of 10 °C min^{-1}. α-[70]PCBM and β-[70]PCBM reveal exothermic peaks at 225 °C and 200 °C attributable to the cold crystallization.[S5]

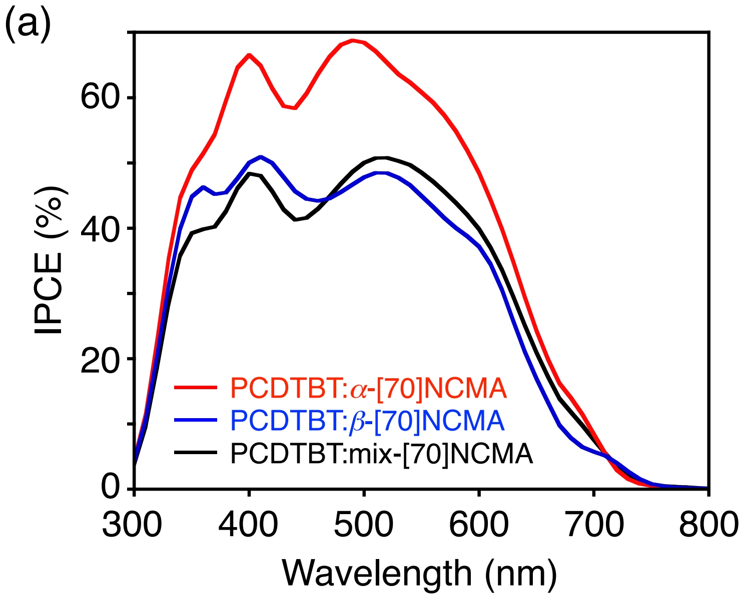

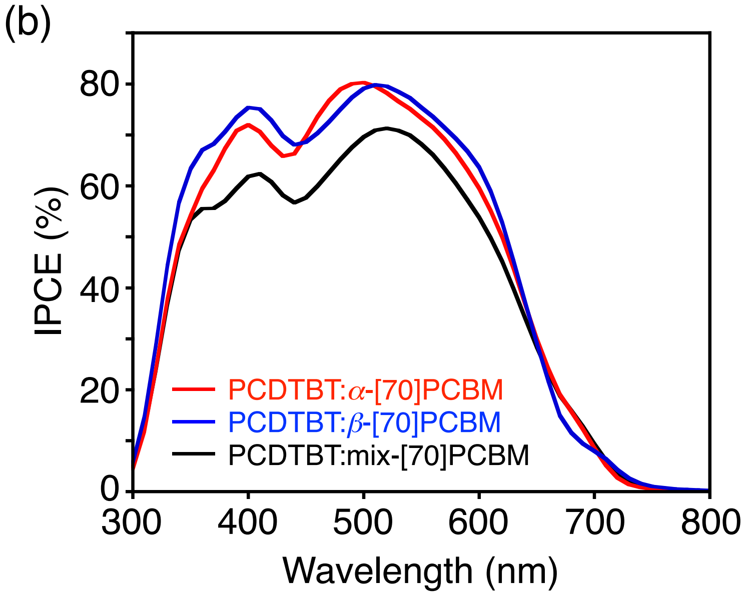

Fig. S8 Photocurrent action spectra of the representative PSC devices based on (c) PCDTBT:α-[70]NCMA (red), PCDTBT:β-[70]NCMA (blue), and PCDTBT:mix-[70]NCMA (black) and (d) PCDTBT:α-[70]PCBM (red), PCDTBT:β-[70]PCBM (blue), and PCDTBT:mix-[70]PCBM (black) films. The convolution of the spectral response with the photon flux of the AM 1.5G spectrum provided the estimated J_{SC} values of (c) 9.96, 7.78, and 7.85 mA cm^{-2} and (d) 12.2, 12.1, and 11.0 mA cm^{-2}, respectively.

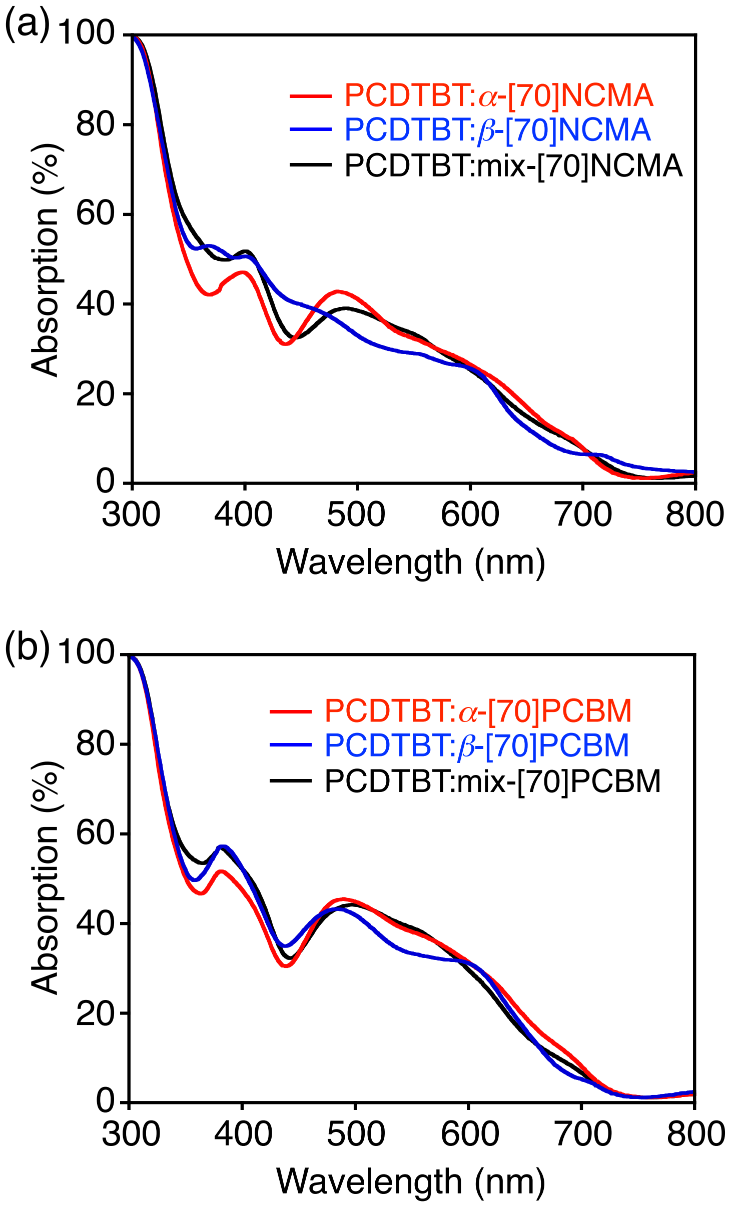

Fig. S9 UV-vis absorption spectra of (a) PCDTBT:*α*-[70]NCMA (red), PCDTBT:*β*-[70]NCMA (blue), and PCDTBT:mix-[70]NCMA (black) and (b) PCDTBT:*α*-[70]PCBM (red), PCDTBT:*β*-[70]PCBM (blue), and PCDTBT:mix-[70]PCBM (black) films. The absorption arising from ITO and PEDOT:PSS was subtracted. Note here that the total absorptions of the ITO/PEDOT:PSS/PCDTBT:fullerene/TiO_x/Al devices are higher than the values in this figure due to the reflection from the Al electrode through the optical spacer, TiO_x.

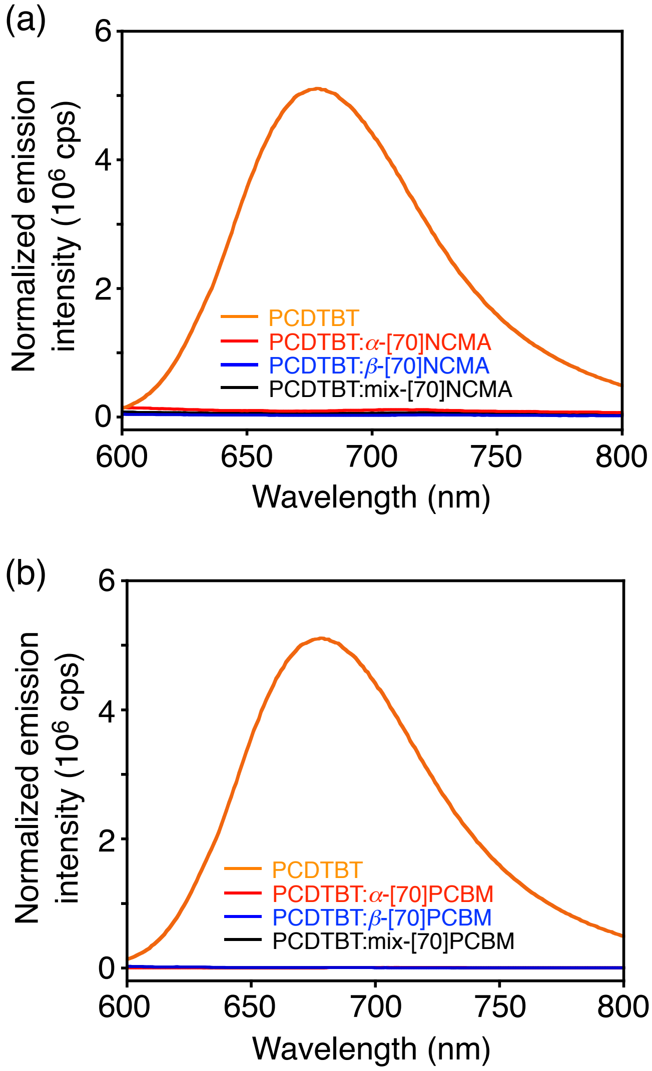

Fig. S10 Photoluminescence spectra of (a) pristine PCDTBT (orange), PCDTBT:α-[70]NCMA (red), PCDTBT:β-[70]NCMA (blue), and PCDTBT:mix-[70]NCMA (black). (b) Pristine PCDTBT (orange), PCDTBT:α-[70]PCBM (red), PCDTBT:β-[70]PCBM (blue), and PCDTBT:mix-[70]PCBM (black) films. The excitation wavelengths are 560 nm. The emission intensities were normalized by that of the PCDTBT film considering the difference in the absorbances of the PCDTBT:fullerene films at the excitation wavelength. The emissions of PCDTBT were quenched almost quantitatively in the blend films. In addition, the excitation of the blend films at 450 nm showed no emissions, suggesting the hot excitons generated in the PCDTBT domain were also quenched by the fullerenes. The fullerene domains were also excited with this higher-energy light, but the emissions from fullerenes were not observed owing to the intrinsic low quantum efficiency.

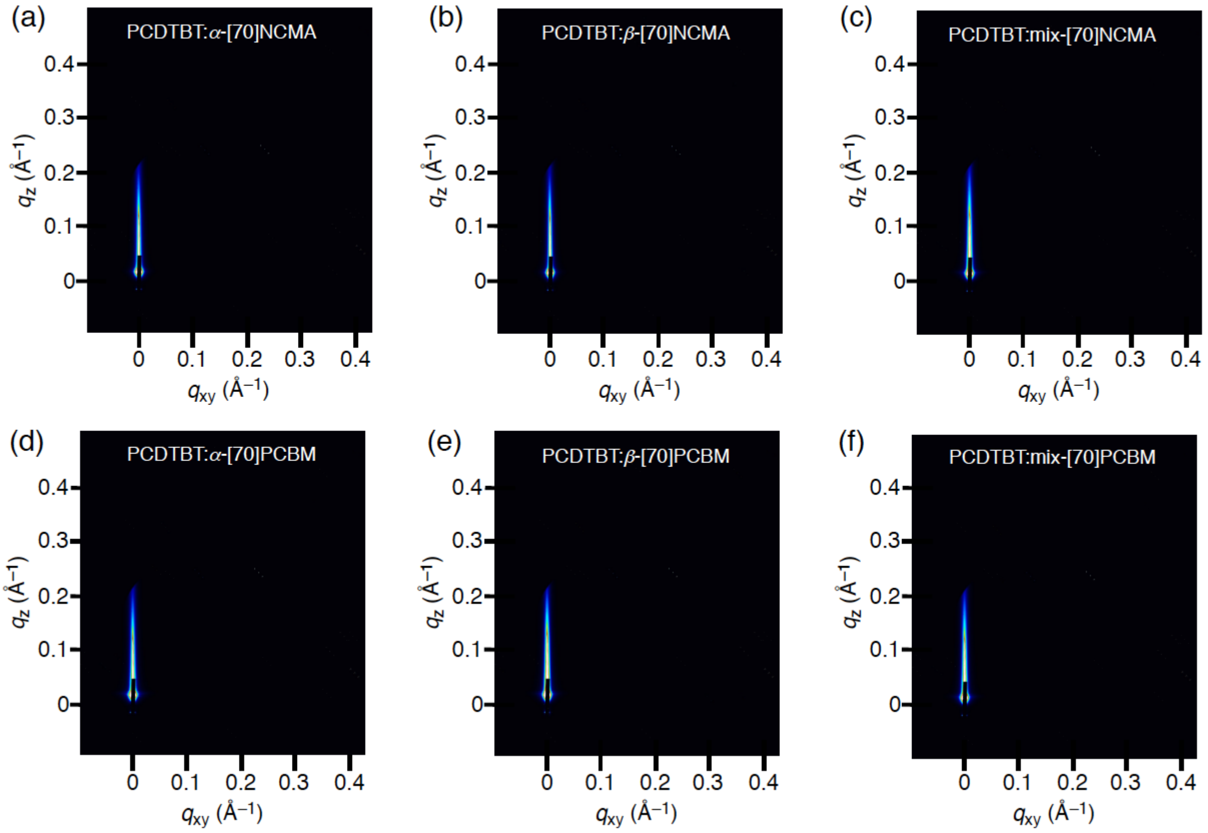

Fig. S11 Two dimensional GISAXS plots of (a) PCDTBT:α-[70]NCMA, (b) PCDTBT:β-[70]NCMA, (c) PCDTBT:mix-[70]NCMA, (d) PCDTBT:α-[70]PCBM, (e) PCDTBT:β-[70]PCBM, and (f) PCDTBT:mix-[70]PCBM films on ITO/PEDOT:PSS substrates.

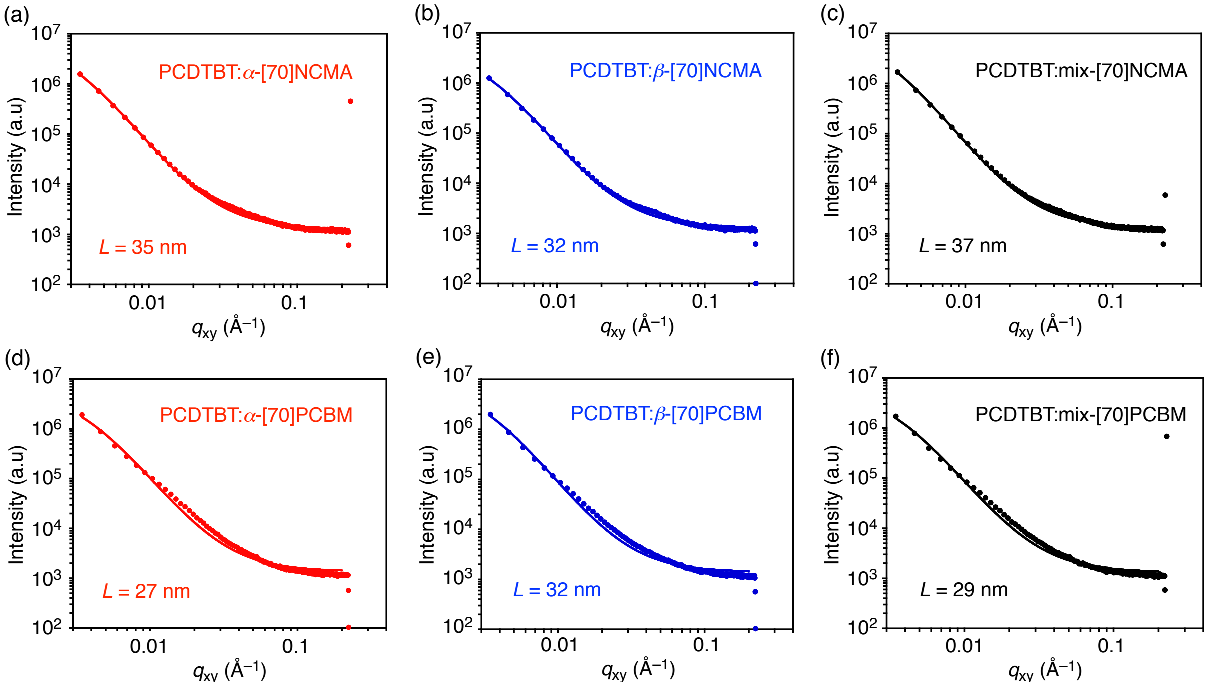

Fig. S12 One dimensional GISAXS profiles of (a) PCDTBT:α-[70]NCMA, (b) PCDTBT:β-[70]NCMA, (c) PCDTBT:mix-[70]NCMA, (d) PCDTBT:α-[70]PCBM, (e) PCDTBT:β-[70]PCBM, and (f) PCDTBT:mix-[70]PCBM films on ITO/PEDOT:PSS substrates. The solid lines represent the Debye-Anderson-Brumberger (DAB) model fittings. The values of correlation lengths L from the fittings are shown as insets.

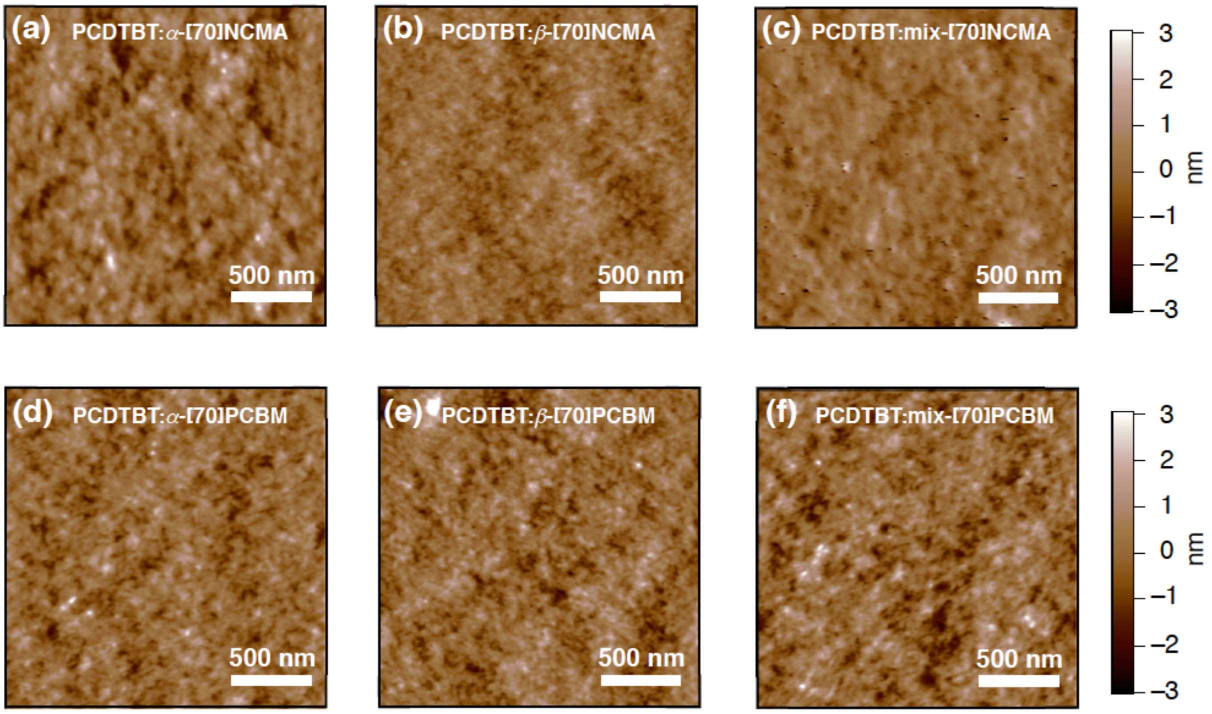

Fig. S13 Tapping-mode AFM images of (a) PCDTBT:α-[70]NCMA, (b) PCDTBT:β-[70]NCMA, (c) PCDTBT:mix-[70]NCMA, (d) PCDTBT:α-[70]PCBM, (e) PCDTBT:β-[70]PCBM, and (f) PCDTBT:mix-[70]PCBM films on ITO/PEDOT:PSS substrates. Scale bars are 500 nm. The colour scale represents the height topography, with bright and dark representing the highest and lowest features, respectively. The rms surface roughnesses are (a) 0.7, (b) 0.6, (c) 0.6, (d) 0.6, (e) 0.7, and (f) 0.7 nm, respectively.

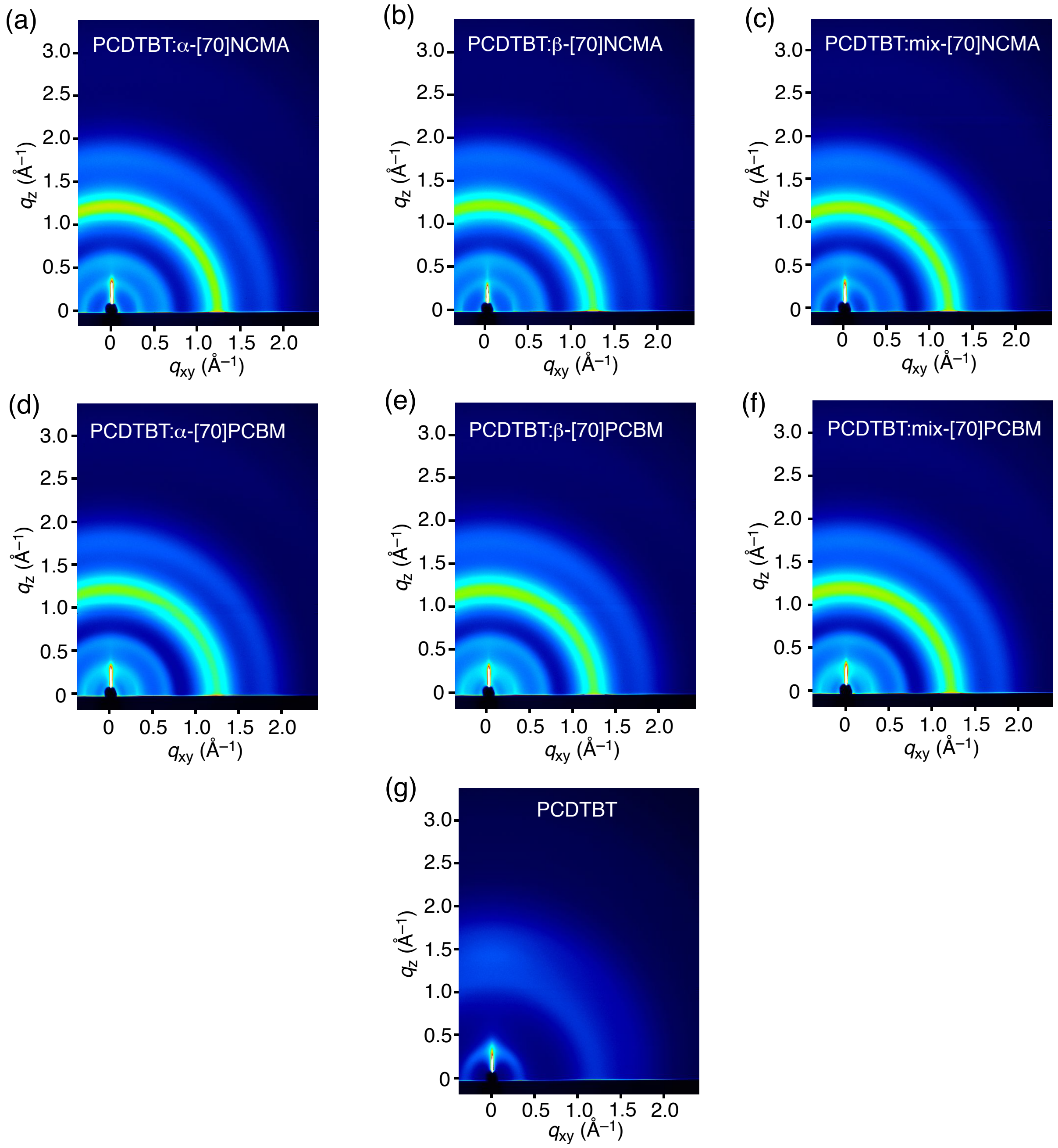

Fig. S14 Two dimensional GIWAXS plots of (a) PCDTBT:α-[70]NCMA, (b) PCDTBT:β-[70]NCMA, (c) PCDTBT:mix-[70]NCMA, (d) PCDTBT:α-[70]PCBM, (e) PCDTBT:β-[70]PCBM, (f) PCDTBT:mix-[70]PCBM, and (g) pristine PCDTBT films on ITO/PEDOT:PSS substrates.

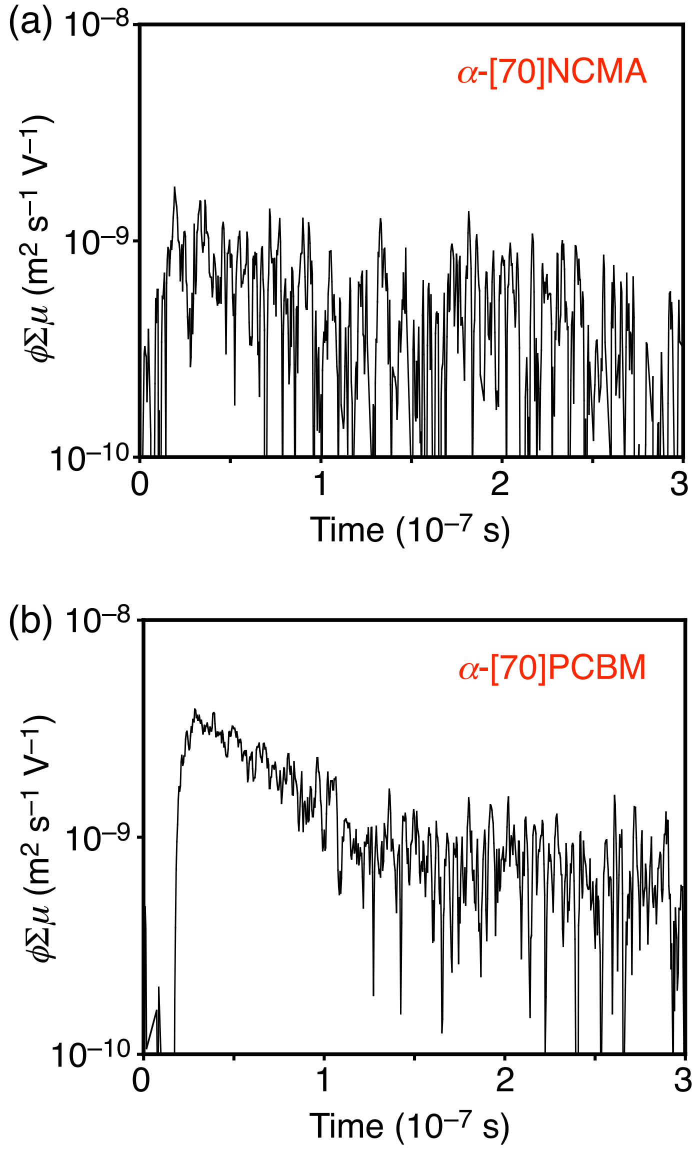

Figure S15. Conductivity transients observed for (a) *α*-[70]NCMA and (b) *α*-[70]PCBM as representative examples. The transients were recorded at an excitation wavelength of 355 nm with a photon density of 4.6×10^{-15} photons cm^{-2}.

Table S1. Reduction potentials.[a]

Fullerene	E_1 / V	E_2 / V	E_3 / V	E_4 / V
α-[70]NCMA	–1.17	–1.55	–1.95	–2.38
β-[70]NCMA	–1.11	–1.50	–1.93	–2.39
mix-[70]NCMA	–1.14	–1.51	–1.90	–2.34
α-[70]PCBM	–1.19	–1.55	–1.96	–2.43
β-[70]PCBM	–1.14	–1.60	–2.03	–2.53
mix-[70]PCBM	–1.17	–1.52	–1.91	–2.33

[a] Values (vs. Fc/Fc^+) were determined by the peak positions in DPV.

Table S2 Averaged device parameters with variation values[a] of BHJPSCs based on PCDTBT:fullerene blend films.

Fullerene	J_{SC} / mA cm^{-2}	V_{OC} / V	FF	PCE / %
α-[70]NCMA	9.40 ± 0.14	0.811 ± 0.004	0.529 ± 0.002	4.04 ± 0.06
β-[70]NCMA	7.14 ± 0.09	0.745 ± 0.006	0.458 ± 0.001	2.44 ± 0.05
mix-[70]NCMA	7.27 ± 0.08	0.765 ± 0.005	0.486 ± 0.001	2.71 ± 0.04
α-[70]PCBM	11.3 ± 0.1	0.804 ± 0.003	0.681 ± 0.003	6.20 ± 0.07
β-[70]PCBM	11.2 ± 0.2	0.847 ± 0.004	0.686 ± 0.006	6.46 ± 0.12
mix-[70]PCBM	10.3 ± 0.1	0.808 ± 0.003	0.672 ± 0.006	5.59 ± 0.08

[a] The photovoltaic parameters were averaged from ten independent solar cells.

References

[S1] N. Haruta, T. Sato and K. Tanaka, *J. Org. Chem.*, 2012, **77**, 9702.

[S2] M. J. Frisch, G. W. Trucks, H. B. Schlegel, G. E. Scuseria, M. A. Robb, J. R. Cheeseman, G. Scalmani, V. Barone, B. Mennucci, G. A. Petersson, H. Nakatsuji, M. Caricato, X. Li, H. P. Hratchian, A. F. Izmaylov, J. Bloino, G. Zheng, J. L. Sonnenberg, M. Hada, M. Ehara, K. Toyota, R. Fukuda, J. Hasegawa, M. Ishida, T. Nakajima, Y. Honda, O. Kitao, H. Nakai, T. Vreven, J. A. Montgomery, Jr., J. E. Peralta, F. Ogliaro, M. Bearpark, J. J. Heyd, E. Brothers, K. N. Kudin, V. N. Staroverov, R. Kobayashi, J. Normand, K. Raghavachari, A. Rendell, J. C. Burant, S. S. Iyengar, J. Tomasi, M. Cossi, N. Rega, J. M. Millam, M. Klene, J. E. Knox, J. B. Cross, V. Bakken, C. Adamo, J. Jaramillo, R. Gomperts, R. E. Stratmann, O. Yazyev, A. J. Austin, R. Cammi, C. Pomelli, J. W. Ochterski, R. L. Martin, K. Morokuma, V. G. Zakrzewski, G. A. Voth, P. Salvador, J. J. Dannenberg, S. Dapprich, A. D. Daniels, Ö. Farkas, J. B. Foresman, J. V. Ortiz, J. Cioslowski and D. J. Fox, Gaussian 09, Gaussian, Inc., Wallingford CT, 2009.

[S3] H.-C. Liao, C.-S. Tsao, T.-H. Lin, C.-M. Chuang, C.-Y. Chen, U. S. Jeng, C.-H. Su, Y.-F. Chen and W.-F. Su, *J. Am. Chem. Soc.*, 2011, **133**, 13064.

[S4] Y.-C. Huang, C.-S. Tsao, C.-M. Chuang, C.-H. Lee, F.-H. Hse, H.-C. Cha, C.-Y. Chen, T.-H. Lin, C.-J. Su, U.-S. Jeng and W.-F. Su, *J. Phys. Chem. C*, 2012, **116**, 10238.

[S5] R. Mens, S. Chambon, S. Bertho, G. Reggers, B. Ruttens, J. D'Haen, J. Manca, R. Carleer, D. Vanderzande and P. Adriaensens, *Magn. Reson. Chem.*, 2011, **49**, 242.